

INVESTIGATION OF FAULT AND ITS EFFECT ON THE BUILD-UP PRESSURE DISTRIBUTION USING NUMERICAL AND ANALYTICAL APPROACHES

Serhii Kryvenko, Arya Shahdi
Texas Tech University

ABSTRACT

The fault effects on the build-up pressure distribution of oil wells were investigated by using numerical and analytical approaches. The limitations and benefits of analytical and numerical solutions of the build-up test were listed in the research. The effects of reservoir boundaries on well responses by using analytical solutions were analyzed. Schlumberger software package "ECLIPSE" was used for the numerical simulation, where the model was discretized to 100 by 100 by 5 grid blocks with the length of each side of the grid block as 75 feet horizontally and 7.5 feet vertically. The model with one production oil well and one injection well with the same characteristics were simulated to prove the well image theory, compare it to the analytical solution and validate the model. The boundary of the reservoir, excluding the fault, was never reached due to the presence of the observation well. Multiple cases, such as one sealing fault, two intersecting faults, semi-permeable faults were analyzed in the model. Horner plots and derivative type curves were built to define the signature of the reservoir. Sensitivity analysis was proposed for each case to provide the correlations between the reservoir parameters. Early time off-trend behavior in build-up test data by using numerical approach was investigated. Semi-permeable fault signature was defined as the decrease of the slope on the derivative type curve after the establishment of the radial flow. The Horner plot in case of two intersecting faults showed the slope four times more than in case of a homogenous reservoir.

INTRODUCTION

Numerical reservoir modeling methods use finite difference approximations, while analytical methods use Boltzman transformation for the solution of diffusivity equation. It leads to certain deviation in the final results of the solution obtained by both methods.

Simple problem that is solved by using the analytical methods requires less time and efforts, comparatively to numerical solution. However, problems solved analytically involve many assumptions, and sometimes cannot be applied for straightforward solution of reservoirs with high heterogeneity, reservoir thickness variations, composite systems, etc.

Pressure transient analysis is one of numerous reservoir engineering areas where numerical solution can be utilized to mimic the reservoir performance. For the purpose of this research we decided to use numerical simulator to simulate the build-up test and compare the results with the analytical solution. Later we added some complexity to the model by adding various types of faults and analyzed the responses of the pressure behavior of the reservoir. More than hundred cases of various sensitivity analysis have been performed for this study.

EFFECT OF RESERVOIR BOUNDARIES ON WELL RESPONSES

To show the effect of the boundaries on the well responses, the simplest example was proposed for the case of one vertical plane - sealing fault located at a certain distance from the well "L". The sequence of pressure regimes in this particular case is the following:

- 1) At the early time, the radius of investigation is smaller than the fault distance L and it corresponds to the infinite acting reservoir (radial flow) (t_1 in the Figure 1).
- 2) Later, the radius of investigation reaches the fault and thus pressure profile deviates from the infinite acting model. (t_2 in the Figure 1). The boundary has been reached and the pressure profile is distorted in the reservoir, but the image curve did not change the well flowing pressure.
- 3) The fault can be seen at the well.
- 4) Hemi-radial flow is reached. The flow lines converge to the well with a half circle geometry. (t_3 in the Figure 1).

During the hemi-radial flow regime, the pressure changes with the logarithm of the elapsed time, while the slope of the semi-log straight line is doubled comparatively to the infinite acting radial flow (Horner, 1951).

Based on the analytical approach, the image well method is used to produce the effect of a no-flow barrier: The image well, at a distance $2L_D$ from the active well, is assumed to be injected with the same flow rate as the producing well. The symmetry condition of the image method requires the use of the same wellbore conditions for both production and injection wells. In most cases, this system can be simplified by using a line source response, expressed with Ei function: $-0.5Ei\left[\frac{-(2L_D)^2}{4t_D}\right]$.

When the distance L_D to the fault is small and the wellbore storage coefficient is high, the fault influence can start during the wellbore storage dominated regime: after the derivative hump, the plateau stabilizes directly at 1, and does not show the first plateau at 0.5. In such a case, the sealing fault is difficult to identify, and the response can be misinterpreted with an infinite acting reservoir.

Similar behavior can be observed on double porosity responses with transient interporosity flow condition. Even though, the responses of the two solutions show a similar shape, the matching procedure will be different. The distance L in the case of one sealing fault can be estimated from the time dt_x , of transition between the two derivative stabilizations, or by matching the data on a computer-generated response.

A sealing fault causes the plateau value to double. With two intersecting faults, the increase of the plateau is correspondingly higher. If a fault is partially sealing, the slope of the derivative curve starts to increase but then falls back to its radial flow value.

Constant pressure boundaries, like a gas cap or aquifer, allow the pressure transient to flatten out at the boundary pressure, so the derivative takes a nosedive, which is easy to recognize. In a closed system, pressure is completely contained within the reservoir. During the Drawdown test, both curves track a line of unit slope, which may be considered as an easily recognizable effect. During the build-up, the derivative curve starts moving toward the line of the unit slope, but takes a nosedive before reaching it. This pattern is very similar to the constant-pressure boundary case.

DESCRIPTION OF THE MODEL PARAMETERS

The model initially has been discretized to 100 by 100 by 5 grid blocks and the length of each side of the grid block is 75 feet horizontally and 7.5 feet vertically. In addition, the location of the well is at the center in order to be as far as possible from the boundaries to make sure we will be in transient zone at all time of the test. The permeability of the reservoir was assumed to be constant

To make sure that the well operates in the transient zone and does not reach the boundary, we decided to place the observation well close to the boundary and make it sensitive to the bottom hole pressure. When bottom hole pressure goes below a certain value, production from the main well will stop to prevent further pressure wave propagation to the boundaries. The used key word is "ACTIONW".

Different distances to the fault was one of the main sensitivity analysis which has been done in this project. However, when the well is too close to the boundaries, it was seen that local grid refinement was needed to better simulate the flow.

The PVT and equilibrium data used in the model is presented in the Table 1. The following parameters were kept unchanged during all simulation runs. Initial reservoir pressure was assumed to be 8000 psi, while the bubble point pressure was set to be 1500 Psi, which excluded the possibility of the two-phase flow. Relative Permeabilities used in the model are shown in the Figure 2 and Figure 3.

EFFECT OF THE FAULT ON THE BUILD-UP TEST

As discussed above, the effect of the fault can be seen in the Horner plot, where the slope of the curve is doubled comparatively to the case with no fault present. At the beginning of the production, the radial flow is observed, with the following hemi-radial flow when the boundary is reached. However if the boundary is located too close to the well, radial flow may be instantaneous, and therefore its effect will be hard to observe on the Horner plot. Therefore, we decided to locate our testing well PROD1 at least 150 feet from the fault. (Figure 4).

In order to verify the image well theory, the injected well INJ1 was located at the distance of 300 feet from the production well. The injection rate was assumed to be equal by modulus to the production rate of PROD1. Our numerical simulations totally confirmed analytical solution, and after performing the build-up test simulation, the observed results had a perfect match for both cases.

The abrupt change of the slope of the curve at the Horner Plot may be used to recalculate the distance of the well to the fault by the following equation:

$$L = \sqrt{\frac{(0.000148)K\Delta t}{\phi\mu c_t}}$$

Build-Up tests for several distances from the well to the fault (300 feet, 450 feet and 600 feet) were simulated. Results obtained validated the equation (Table 2). Minor differences may be due to the subjectivism of the selection of the spot on the curve, where the slope of the Horner plot deviates, indicating the beginning of the hemi-radial flow.

Limitations of the Horner plot to clearly observe the flow transition, and therefore the indication of flow boundaries led us to use log-log derivative curves too for next sensitivity analyses. After we have verified, the analytical solution theory with the finite difference approximations, we decided to look at more comprehensive examples.

Another sensitivity analysis is done for the case of crossing faults with different degrees and distances. There is a logical argument stating that pseudo steady state flow regime is present because of the influence of two of the flow boundaries. The Horner plot in case of two perpendicularly intersecting faults showed the slope of four times more than in case of a homogenous reservoir (Figure 5). It is important to mention that Horner build-up plot should not be used for multiple faults distance calculations in case of non-bisector position of the well. Instead, the Tiab and Kumar solution must be applied.

Sensitivity analysis in case of the leaking fault was performed and revealed the following trend (, presented below for both infinite conductive and finite conductive faults (Figure 7). The transmissibility ratio was changed in Eclipse in order to assign the properties of the fault

$$\alpha = \frac{k_f/w_f}{k/L}$$

Infinite conductivity fault: $\alpha < 1$

Finite conductivity fault: $\alpha > 1$

As it can be seen from the graph, in case of $a=2$, the derivative curve follows similar to radial flow pattern.

The pressure distribution of the reservoir for the cases stated above is shown on the Figure 8.

WAY FORWARD

The work presented in this project includes the effects of fault on the build-up test, assuming the rest conditions are homogenous. That is why in order to improve our model, more sensitivity analysis should be proposed. More signatures should be added, such as:

- 1) The effect of the skin
- 2) Various geometry of the fault(s)
- 3) Partially penetrated well
- 4) Double porosity reservoir
- 5) Double permeability reservoir
- 6) Multiphase flow
- 7) Tight reservoir
- 8) Application of the model to a real field

CONCLUSIONS

- 1) ECLIPSE build-up test implementation was proved by recalculating the permeability from the generated pressure data (using Horner plot) and showed the same value as assigned one.
- 2) When there is no fault present, the concavity is downward however, with fault, the concavity is upward.
- 3) The image well theory was validated and showed exactly the same trend and behavior as "with fault" case.
- 4) The time associated with slope change can be used to determine the fault distance from the well.
- 5) Early time data shows an off-trend behavior in build-up test data.
- 6) The boundary of the reservoir (another than fault) in the model is never reached due to the presence of the observation well.
- 7) Derivative type curve was applied to identify the signature of the reservoir for three different scenarios: one sealing fault, two intersecting faults, one semi-permeable fault.

- 8) The increase of the slope is observed in case of two intersecting sealing faults, comparatively to one sealing fault (both on the Horner plot and derivative type curve).
- 9) Semi-permeable fault signature is the decrease of the slope on the log-log plot after the radial flow is established.

REFERENCES

1. Lee, J., 1982. Well Testing. Textbook Series, Vol.1, Society of Petroleum Engineers of AIME, Dallas.
2. Blasingame, T.A., Johnston, L.L., Rushing, J. A., 1990. Pressure Integral Type-Curves analysis-II: Applications and Field Cases.
3. Bourdet, D. Ayoub, J.A. and Pirard, Y. M., 1989. Use of Pressure Derivative in Well-Test Interpretation. SPEFE, June,293-302
4. Horner, D. R., 1951. Pressure Build-ups in Wells. Proc., Third World Pet. Cong.
5. Grey, K.E., 1965. Approximating Well-to Fault Distance From Pressure Build-up Test.
6. Tarek, A. "Reservoir Engineering Handbook", Third Edition, Gulf Professional Publishing, 2006.

LIST OF TABLES AND FIGURES

Table 1: PVT and Equilibrium Properties of the model

Property	Value
Initial Reservoir Pressure	8000 psi
Bubble Point Pressure	1500 psi
Reference Pressure	3600 psi
Oil viscosity	0.4 cp
Oil density	40 lb/ft ³
Water density	62 lb/ft ³
Gas density	0.07773 lb/ft ³
Water Formation Volume Factor	1 bbl/STB
Oil Formation Volume Factor	1.1 bbl/STB

Table 2: Assigned and Calculated Distance from PROD1 to the fault

Assigned distance from the PROD1 to the Vertical Sealing Fault	The start of the hemi-radial flow $\frac{t_p + \Delta t}{\Delta t}$	Δt	Calculated distance from the PROD1 to the Vertical Sealing Fault
300 feet	4.8	31.58	303.15 feet
450 feet	3.3	52.17	455.16 feet
600 feet	2	120	593.89 feet

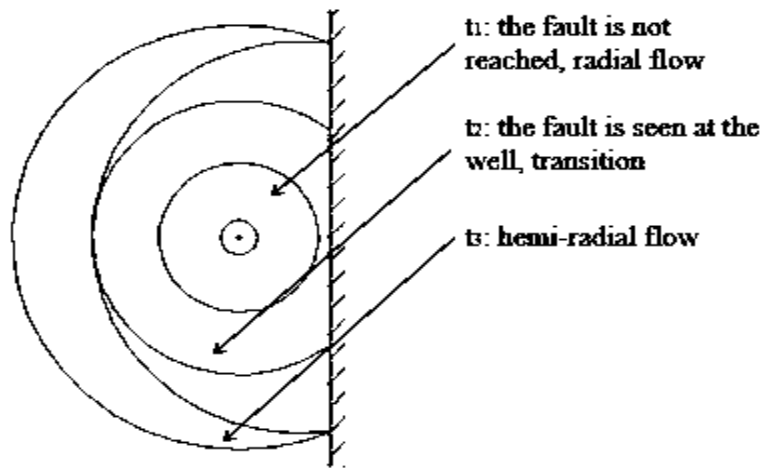


Figure 1 – Effect of reservoir boundaries on well response

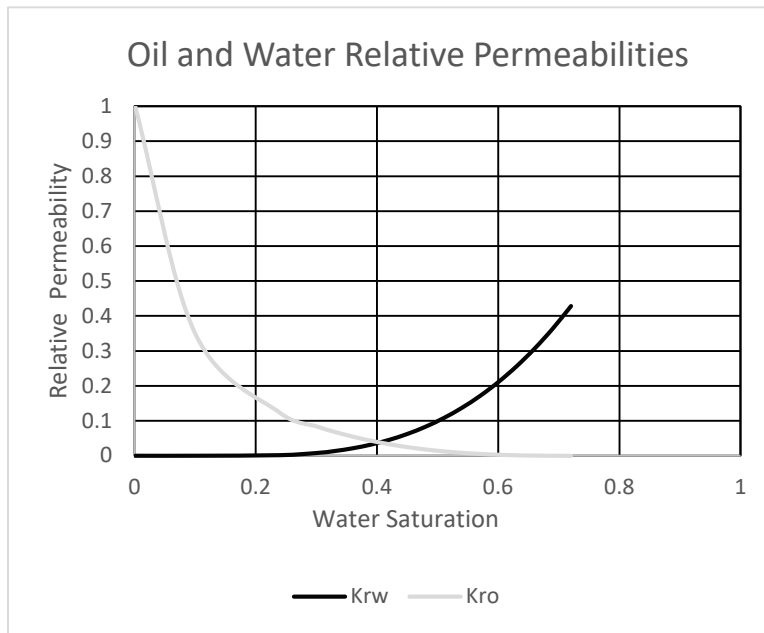


Figure 2 – Relative Permeabilities of Oil and Water

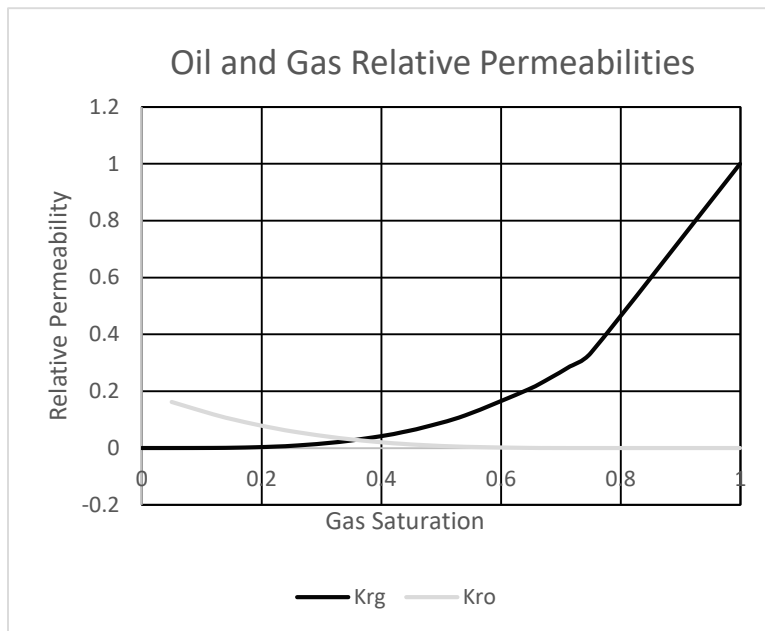


Figure 3– Relative Permeabilities of Oil and Gas

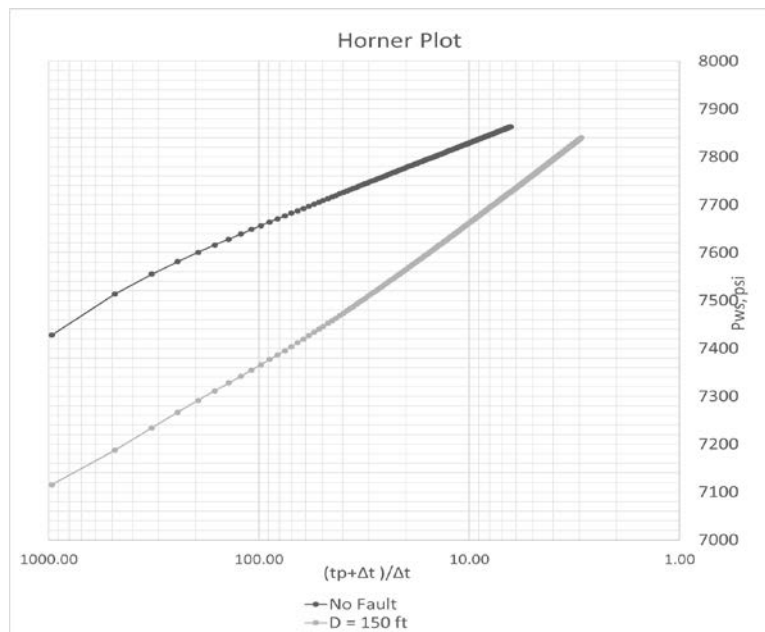


Figure 4 – Horner Plot in case of one sealing fault

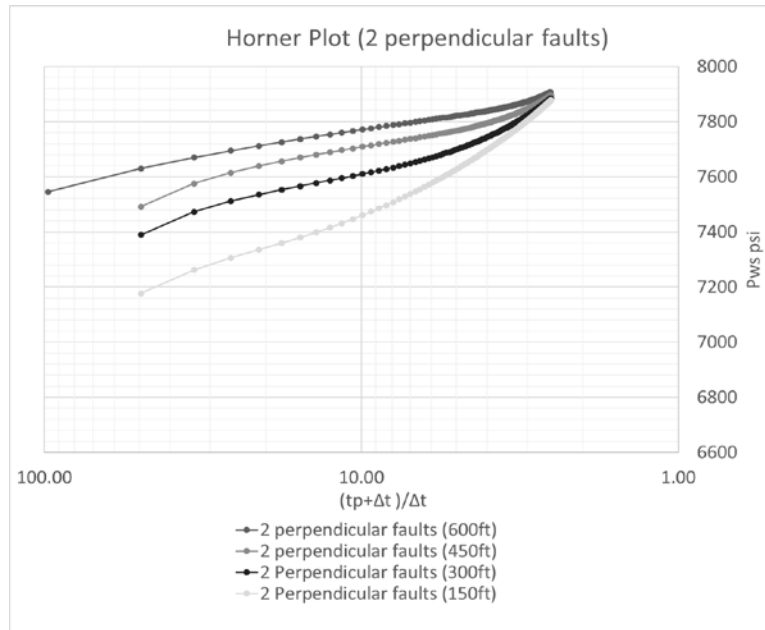


Figure 5 – Horner Plot in case of two intersecting perpendicular faults

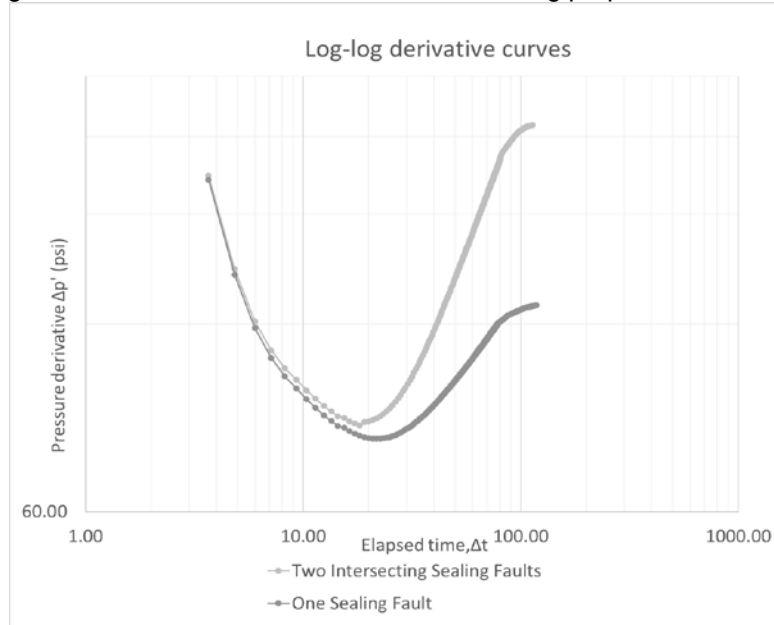


Figure 6 – Log-log derivative curve in case of two intersecting perpendicular sealing faults

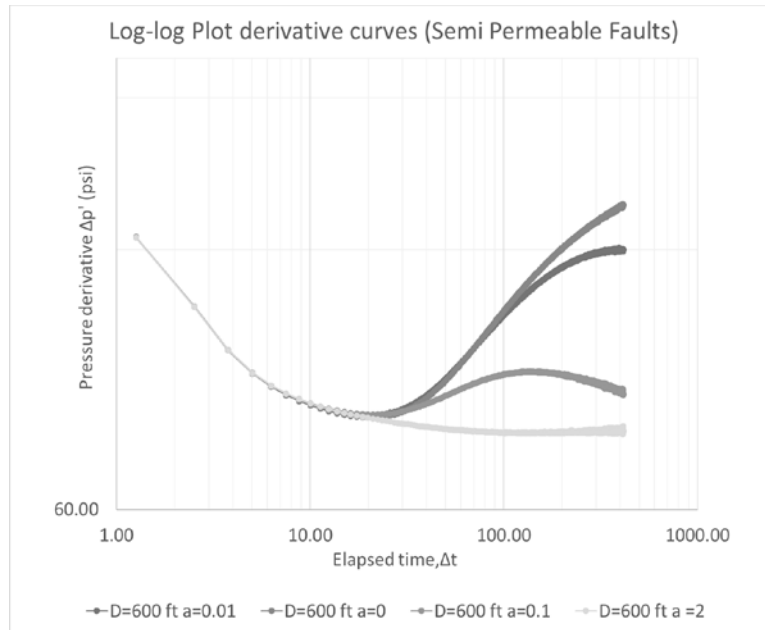


Figure 7 – Log-log derivative curve in case of semi-permeable faults

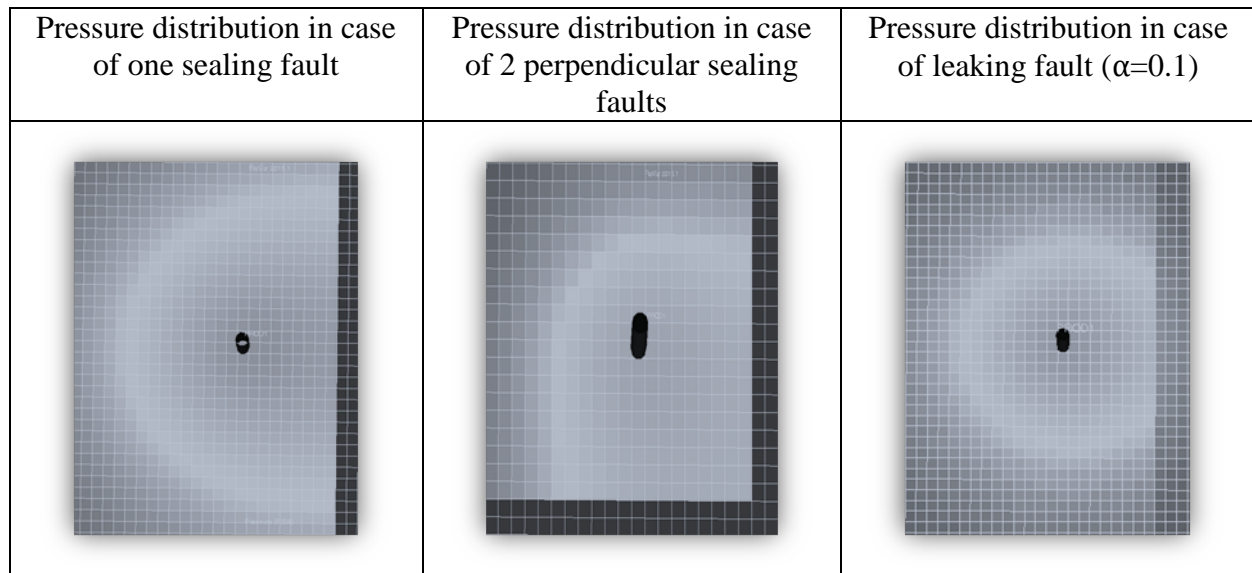


Figure 8 – Pressure Distribution Profiles from the Floviz